Available online at www.sciencedirect.com

ScienceDirect

Journal of Sound and Vibration 319 (2009) 850–868

JOURNAL OF SOUND AND VIBRATION

www.elsevier.com/locate/jsvi

A time-varying identification method for mixed response measurements

Timothy C. Allison[a,*], A. Keith Miller[b], Daniel J. Inman[c]

[a]Southwest Research Institute, 6220 Culebra Road, San Antonio, TX 78238, USA
[b]Sandia National Laboratories, P.O. Box 5800, Albuquerque, NM 87195-0847, USA
[c]Virginia Polytechnic Institute and State University, 310 Durham Hall, MC 0261, Blacksburg, VA 24061, USA

Received 11 October 2007; received in revised form 9 June 2008; accepted 20 June 2008
Handling Editor: S. Bolton
Available online 29 July 2008

Abstract

The proper orthogonal decomposition is a method that may be applied to linear and nonlinear structures for extracting important information from a measured structural response. This method is often applied for model reduction of linear and nonlinear systems and has been applied recently for time-varying system identification. Although methods have previously been developed to identify time-varying models for simple linear and nonlinear structures using the proper orthogonal decomposition of a measured structural response, the application of these methods has been limited to cases where the excitation is either an initial condition or an applied load but not a combination of the two. This paper presents a method for combining previously published proper orthogonal decomposition-based identification techniques for strictly free or strictly forced systems to identify predictive models for a system when only mixed response data are available, i.e. response data resulting from initial conditions and loads that are applied together. This method extends the applicability of the previous proper orthogonal decomposition-based identification techniques to operational data acquired outside of a controlled laboratory setting. The method is applied to response data generated by finite element models of simple linear time-invariant, time-varying, and nonlinear beams and the strengths and weaknesses of the method are discussed.

1. Introduction

The finite element method is commonly used to analyze the dynamics of complex structures [1]. Although the method is very powerful and its extensive use in analyses is justified, some of its limitations become apparent when it is applied for analysis of very large, possibly nonlinear structures with millions of degrees of freedom. Months may be required to develop the geometry and form the element mesh for such models. After the model is completed the analysis may require days or weeks of processing time [2]. Finally, there is no guarantee that the analysis will accurately predict behavior of an actual structure. The analysis may be incorrect due to modeling errors (e.g., incorrect assumptions about damping or linearity), parameter errors

*Corresponding author. Tel.: +1 210 522 3561.
E-mail addresses: talliso@vt.edu, tim.allison@swri.org (T.C. Allison).

0022-460X/$ - see front matter
doi:10.1016/j.jsv.2008.06.031

(e.g., inaccuracy of Young's modulus), or other factors [3]. For this reason, model updating and validation procedures are often employed to ensure that the model accurately produces results that are consistent with experimental measurements.

Many system identification methods have been developed that use experimental response data to improve or create numerical modes for structures. For example, modal analysis is commonly used to compare resonant frequencies and/or mode shapes of linear time-invariant finite element models with experimental results [4]. Model updating is also considered a type of system identification because it applies experimental data to improve the numerical model [5]. Other system identification methods have been developed for linear and nonlinear systems that attempt to develop a numerical model from the data when no finite element model is available. However, current nonlinear identification techniques are only developed for systems where the functional form of the nonlinearity can be determined from the data. Because a large variety of nonlinear forms exist, the process of characterizing nonlinearities is difficult and cannot always be accomplished. The requirement that nonlinear forms must be known, then, represents a significant drawback to nonlinear identification theory.

Linear time-varying systems may be well-suited to model the behavior of nonlinear systems and time-varying system identification has been proposed as an alternative to nonlinear system identification [6], but most linear time-varying identification methods require a prior understanding of the functional form of the time variance. A general method for time-varying system identification was proposed for biological systems in Ref. [7], but its application is limited to single-input single-output systems and a large number of data sets are required. Perhaps due to these limitations, linear time-varying methods have not yet been applied for nonlinear system identification.

Recent research has developed methods for time-varying identification of multiple-input multiple-output structural systems based on the proper orthogonal decomposition [8,9]. Unfortunately, these methods can only be applied to situations where the system is excited by either an initial condition or an applied load, but not a combination of the two. In a non-laboratory setting it may be impractical to eliminate applied loads or initial conditions (i.e. the structure may never be at rest). This paper presents a method for combining previous proper orthogonal decomposition-based identification techniques so that they may be applied in situations where strictly free or strictly forced responses are unobtainable, only a combination of the two.

The proper orthogonal decomposition is a statistical tool for extracting dominant information from experimental data. The proper orthogonal decomposition has been applied in a variety of fields such as fluid mechanics, economics, heat transfer, and, recently, structural dynamics [10]. The proper orthogonal decomposition is attractive because it can be applied to any linear or nonlinear system to express a measured response as a summation of modes [3]. These modes are generally different from the familiar eigenmodes of a (linear time-invariant) system and can represent the measured response (even for a nonlinear system) to any desired degree of accuracy by using enough dominant modes. The proper orthogonal decomposition is a linear procedure but it does "not do the physical violence of linearization methods" and has been referred to as a "safe haven in the intimidating world of nonlinearity" [11]. The system identification methods proposed in Refs. [8,9] and also in this paper use the proper orthogonal decomposition to cast a measured response into the framework of a modal sum. Ideas from linear system theory and mode summation theory are then applied to develop methods for using the data in the proper orthogonal decomposition to express the response of the system to new excitations.

This paper is organized into six sections including this introduction. The following section provides an overview of the proper orthogonal decomposition and its computation from the singular value decomposition of a snapshot matrix. The next section reviews previously published methods of proper orthogonal decomposition-based system identification for strictly free or strictly forced responses. This is followed by the description of a method to combine free- and forced-response methods for mixed responses. Next, examples are given using finite element models of linear time-invariant, time-varying, and nonlinear beams. Finally, we present conclusions about the strengths and weaknesses of the proposed method.

2. The proper orthogonal decomposition

The proper orthogonal decomposition can be computed by several methods [10]. This section explains how the proper orthogonal decomposition is computed with the singular value decomposition of a snapshot matrix. First, a system response is generated by exciting the system by applying a load or imposing an initial condition, or both simultaneously. Next, the displacement at m degrees of freedom is sampled n times and the data are arranged in a "snapshot" matrix $\mathbf{W}$:

$$\mathbf{W} = \begin{bmatrix} w_1(t_1) & w_1(t_2) & \cdots & w_1(t_n) \\ w_2(t_1) & w_2(t_2) & & \\ \vdots & & \ddots & \\ w_m(t_1) & & & w_m(t_n) \end{bmatrix}. \tag{1}$$

Next, the singular value decomposition of $\mathbf{W}$ is computed:

$$\mathbf{W} = \mathbf{U}\mathbf{\Sigma}\mathbf{V}^{\mathrm{T}}. \tag{2}$$

In Eq. (2), the columns $\mathbf{u}_i$ of $\mathbf{U}$ are the proper orthogonal modes, the columns $\mathbf{v}_i$ of $\mathbf{V}$ are the proper orthogonal coordinate histories that correspond to each proper orthogonal mode, and $\mathbf{\Sigma}$ is a diagonal matrix whose diagonal elements σ_i are the proper orthogonal values corresponding to each proper orthogonal mode. The proper orthogonal coordinate histories describe the amplitude modulation of each proper orthogonal mode and the proper orthogonal values describe the relative significance of each proper orthogonal mode in the response $\mathbf{W}$ [10,12]. If the system is linear and lightly damped with a mass matrix proportional to the identity matrix then the proper orthogonal modes will be equal to the linear normal modes [13,14]. For nonlinear systems if a single nonlinear normal mode is excited then the first proper orthogonal mode is a linear approximation to the excited nonlinear normal mode [13,15]. The percentage of signal energy captured by a single proper orthogonal mode $\mathbf{u}_i$ is given by

$$\varepsilon_i = \frac{\sigma_i}{\sum_{j=1}^{m} \sigma_j}. \tag{3}$$

Typically, only proper orthogonal modes that constitute a certain percentage of signal energy (e.g. 99% or 99.9%) are considered [10,12]. If k dominant proper orthogonal modes are considered then we may approximate $\mathbf{W}$ as a summation of proper orthogonal modes and corresponding proper orthogonal coordinate histories, shown below (noting that $\mathbf{\Sigma}$ is diagonal):

$$\mathbf{W} \approx \sum_{i=1}^{k} \sigma_i \mathbf{u}_i \mathbf{v}_i^{\mathrm{T}}. \tag{4}$$

We note that even signals generated by nonlinear systems may be represented by a summation of proper orthogonal modes. The proper orthogonal modes are "appealing for nonlinear system identification", in part because they "obey a 'sort of principle of superposition' due to the fact that the original signal is retrieved when all of the modal contributions are added up" [3]. In addition, the proper orthogonal modes are the optimal basis for reconstructing the original displacement efficiently. In other words, $\mathbf{W}$ may be approximated using fewer proper orthogonal modes than any other modes while maintaining the same level of accuracy. Finally, it should be noted that the proper orthogonal modes and coordinate histories are orthonormal:

$$\mathbf{U}^{\mathrm{T}}\mathbf{U} = \mathbf{V}^{\mathrm{T}}\mathbf{V} = \mathbf{I}. \tag{5}$$

Although this section has focused on calculation of the proper orthogonal modes, values, and coordinate histories by performing a singular value decomposition, these quantities may also be determined when calculating the proper orthogonal decomposition by other methods [10]. The singular value decomposition is used in this instance for its simplicity and convenient expression as a summation of modes.

3. Proper orthogonal decomposition-based system identification

This section introduces the proper orthogonal decomposition-based system identification techniques for strictly free and strictly forced response from Refs. [8,9]. First, an analytical expression for the proper orthogonal coordinate histories is developed using mode summation and linear system theory. Then, this expression is manipulated for identification and response prediction of systems excited by initial conditions and loads, respectively.

3.1. Expression for proper orthogonal coordinate histories

The displacement $w(x, t)$ of a vibratory system is governed by the (generally time-varying) equation

$$M\{\ddot{w}, t\} + D\{\dot{w}, t\} + L\{w, t\} = f(x, t), \tag{6}$$

where M, D, and L are mass, damping, and stiffness operators, respectively, and $f(x, t)$ is a distributed forcing function. At this point we do not make any assumptions about the form of M, D, and L other than that they are linear. The solution to Eq. (6) may be computed by approximating the displacement variable with a modal sum:

$$w(x, t) \approx \sum_{i=1}^{k} u_i(x) v_i(t). \tag{7}$$

In this paper we assume that the proper orthogonal modes are used as the modes $u_i(x)$. If this is the case then the modal coordinates $v_i(x)$ are equivalent to the proper orthogonal coordinates scaled by the proper orthogonal values. In other words, the scaled proper orthogonal coordinate histories $\hat{\mathbf{v}}_i = \sigma_i \mathbf{v}_i$ are time-sampled forms of the modal coordinates. We may then combine Eqs. (6) and (7) to obtain a matrix ordinary differential equation for the proper orthogonal coordinates:

$$\mathbf{M}(t)\ddot{\mathbf{v}}(t) + \mathbf{D}(t)\dot{\mathbf{v}}(t) + \mathbf{K}(t)\mathbf{v}(t) = \mathbf{q}(t). \tag{8}$$

In Eq. (8), the quantities $\mathbf{M}(t)$, $\mathbf{D}(t)$, and $\mathbf{K}(t)$ are the mass, damping, and stiffness matrices formed by taking inner products of the proper orthogonal modes with the respective operators [16]. The quantity $\mathbf{q}(t)$ is a vector of modal forces obtained by forming the inner product of the proper orthogonal modes with the applied load $f(x, t)$. In general, the matrices in Eq. (8) are full and an expression for the proper orthogonal coordinates is found by converting Eq. (8) to state form:

$$\begin{Bmatrix} \dot{\mathbf{v}}(t) \\ \ddot{\mathbf{v}}(t) \end{Bmatrix} = \mathbf{A}(t) \begin{Bmatrix} \mathbf{v}(t) \\ \dot{\mathbf{v}}(t) \end{Bmatrix} + \mathbf{B}(t)\mathbf{q}(t). \tag{9}$$

In Eq. (9), $\mathbf{A}(t)$ and $\mathbf{B}(t)$ are state matrices formed from $\mathbf{M}(t)$, $\mathbf{D}(t)$, and $\mathbf{K}(t)$:

$$\mathbf{A}(t) = \begin{bmatrix} \mathbf{0} & \mathbf{I} \\ -\mathbf{M}(t)^{-1}\mathbf{K}(t) & -\mathbf{M}(t)^{-1}\mathbf{D}(t) \end{bmatrix}, \tag{10}$$

$$B(t) = \begin{bmatrix} \mathbf{0} \\ \mathbf{M}(t)^{-1} \end{bmatrix}. \tag{11}$$

The solution to Eq. (9) is given by [16]:

$$\begin{Bmatrix} \mathbf{v}(t) \\ \dot{\mathbf{v}}(t) \end{Bmatrix} = \mathbf{\Phi}(t) \begin{Bmatrix} \mathbf{v}(0) \\ \dot{\mathbf{v}}(0) \end{Bmatrix} + \int_0^t \mathbf{\Phi}(t-\tau)\mathbf{B}(t-\tau)\mathbf{q}(\tau)\mathrm{d}\tau, \tag{12}$$

where $\mathbf{\Phi}(t)$ is the state transition matrix, which for time-varying systems can be computed from the Peano–Baker series [17]:

$$\mathbf{\Phi}(t) = \mathbf{I} + \int_0^t \mathbf{A}(\sigma_1)\,\mathrm{d}\sigma_1 + \int_0^t \mathbf{A}(\sigma_1) \int_0^{\sigma_1} \mathbf{A}(\sigma_2)\,\mathrm{d}\sigma_2\,\mathrm{d}\sigma_1 + \dots . \tag{13}$$

The scaled proper orthogonal coordinate histories are obtained from the upper-half partition of Eq. (12), i.e.

$$\mathbf{v}(t) = [\mathbf{\Phi}_{11}(t) \quad \mathbf{\Phi}_{12}(t)] \begin{Bmatrix} \mathbf{v}(0) \\ \dot{\mathbf{v}}(0) \end{Bmatrix} + \int_0^t \mathbf{\Phi}_{12}(t-\tau)\mathbf{M}^{-1}(t-\tau)\mathbf{q}(\tau)\,\mathrm{d}\tau, \tag{14}$$

where $\mathbf{\Phi}(t)$ is partitioned into four equal submatrices:

$$\mathbf{\Phi}(t) = \begin{bmatrix} \mathbf{\Phi}_{11}(t) & \mathbf{\Phi}_{12}(t) \\ \mathbf{\Phi}_{21}(t) & \mathbf{\Phi}_{22}(t) \end{bmatrix}. \tag{15}$$

If a system is linear, lightly damped, has a mass matrix proportional to the identity matrix, and is responding to initial conditions only, then the proper orthogonal modes are equivalent to the eigenmodes of the system [13,14] and the mass and stiffness matrices in Eq. (8) are diagonal. If proportional damping exists, then the damping matrix is also diagonal and the state matrix $\mathbf{A}(t)$ is a block matrix composed of four equally sized submatrices that are diagonal. If $\mathbf{A}(t)$ is composed of diagonal submatrices, then so are all of the integrals of $\mathbf{A}(t)$ and matrix products of $\mathbf{A}(t)$ with its integrals in Eq. (13). Because every term in Eq. (13) is composed of diagonal submatrices, then the submatrices of $\mathbf{\Phi}(t)$ in Eq. (15) are all diagonal.

An example is now presented of a system that meets the requirements for the proper orthogonal modes to be equal to the eigenmodes. Consider the nondimensional mass-spring system shown in Fig. 1.

The mass matrix for the system is

$$\mathbf{M} = \begin{bmatrix} 1 & 0 & 0 \\ 0 & 1 & 0 \\ 0 & 0 & 1 \end{bmatrix}$$

and the stiffness matrix is

$$\mathbf{K} = \begin{bmatrix} 2 & -1 & 0 \\ -1 & 2 & -1 \\ 0 & -1 & 1 \end{bmatrix}.$$

This system is undamped and the mass matrix is proportional to (in fact, it is equal to) the identity matrix. The eigenmodes (scaled so that they are orthonormal) for the system are

$$[\,\boldsymbol{\psi}_1 \quad \boldsymbol{\psi}_2 \quad \boldsymbol{\psi}_3\,] = \begin{bmatrix} 0.328 & 0.737 & -0.591 \\ 0.591 & 0.328 & 0.737 \\ 0.737 & -0.591 & -0.328 \end{bmatrix}.$$

The system is given an initial displacement of $\mathbf{w}_0 = [\,0 \quad 0 \quad 1\,]^{\mathrm{T}}$ and the response is sampled every 0.1 s for 120 s. The proper orthogonal modes for the system may be computed from the measured response and are equal to

$$[\,\mathbf{u}_3 \quad \mathbf{u}_1 \quad \mathbf{u}_2\,] = \begin{bmatrix} 0.3246 & 0.7398 & -0.5893 \\ 0.5836 & 0.3337 & 0.7403 \\ 0.7443 & -0.5843 & -0.3235 \end{bmatrix}.$$

We note that the order of the proper orthogonal modes is not the same as that of the eigenmodes. This is because the third eigenmode is most active in the measured response and is therefore approximated by the proper orthogonal mode that corresponds to the highest proper orthogonal value, i.e. the first proper orthogonal mode. The proper orthogonal modes and eigenmodes, although very similar, are not exactly equal. However, the study in Ref. [13] demonstrated empirically that the difference in proper orthogonal modes and

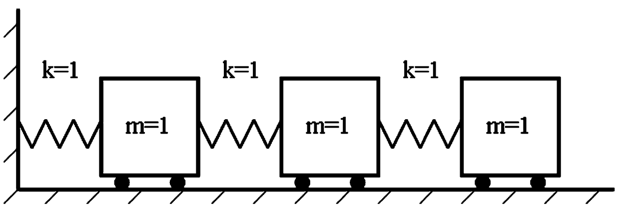

Fig. 1. Example mass-spring system with equal masses.

eigenmodes disappears as number of samples and the total measurement time increase. In this case, we will show that the proper orthogonal modes and eigenmodes are similar enough that the assumption of diagonal submatrices of $\mathbf{\Phi}(t)$ holds. The proper orthogonal-modal mass and stiffness matrices are calculated to be

$$\mathbf{M}' = \begin{bmatrix} 1 & 0 & 0 \\ 0 & 1 & 0 \\ 0 & 0 & 1 \end{bmatrix},$$

$$\mathbf{K}' = \begin{bmatrix} 1.5546 & 0.0004 & 0.0126 \\ 0.0004 & 3.2469 & 0.0178 \\ 0.0126 & 0.0178 & 0.1983 \end{bmatrix}.$$

We note that although the modal stiffness matrix is not diagonal, it is diagonally dominant. The modal matrices may now be used to form the state matrix $\mathbf{A}$:

$$\mathbf{A} = \begin{bmatrix} \mathbf{0}_{3\times3} & \mathbf{I}_{3\times3} \\ -\mathbf{K}' & \mathbf{0}_{3\times3} \end{bmatrix}.$$

Finally, the state transition matrix $\mathbf{\Phi}(t)$ may be formed at every time step from the series in Eq. (13). Although it is impractical here to show all of the data at multiple time steps, we can illustrate the diagonal dominance of the various submatrices of $\mathbf{\Phi}(t)$ by examining the 2-norm of each matrix element over a time range. The values of each element of $\mathbf{\Phi}(t)$ were calculated at every 0.1 s for 10 s and a vector was formed containing the time-series data for each matrix element, i.e.

$$\mathbf{p}_{ij} = \begin{bmatrix} \mathbf{\Phi}_{ij}(t_1) \\ \mathbf{\Phi}_{ij}(t_2) \\ \vdots \\ \mathbf{\Phi}_{ij}(t_{100}) \end{bmatrix}.$$

The 2-norm of each vector $\mathbf{p}_{ij}$ was then calculated. The 2-norms for each element of $\mathbf{\Phi}(t)$ are shown below:

$$\begin{bmatrix} ||\mathbf{p}_{11}||_2 & ||\mathbf{p}_{12}||_2 & \cdots & ||\mathbf{p}_{16}||_2 \\ ||\mathbf{p}_{21}||_2 & ||\mathbf{p}_{22}||_2 & & \\ \vdots & & \ddots & \\ ||\mathbf{p}_{61}||_2 & & & ||\mathbf{p}_{66}||_2 \end{bmatrix} = \begin{bmatrix} 50.60 & 0.00 & 0.01 & 32.40 & 0.00 & 0.02 \\ 0.00 & 49.36 & 0.00 & 0.00 & 15.90 & 0.01 \\ 0.01 & 0.00 & 53.33 & 0.02 & 0.01 & 240.57 \\ 78.34 & 0.00 & 0.01 & 50.60 & 0.00 & 0.01 \\ 0.00 & 167.66 & 0.01 & 0.00 & 49.36 & 0.00 \\ 0.01 & 0.01 & 9.44 & 0.01 & 0.00 & 53.33 \end{bmatrix}.$$

Clearly, the diagonal terms in each of the four submatrices of $\mathbf{\Phi}(t)$ contain much larger values than the off-diagonal terms. The proposed method assumes that the proper orthogonal modes diagonalize the modal matrices of the system, and is valid for unforced systems that are lightly damped with a mass matrix proportional to the identity matrix. Even in cases where the proper orthogonal modes do not exactly diagonalize the system's modal matrices, the modal matrices may be diagonally dominant and the approximation may still be accurate.

3.2. Free response identification

If the snapshot matrix $\mathbf{W}$ is formed from the response to an initial displacement profile $\mathbf{w}_0$, then the snapshot matrix for the response to a new initial displacement profile $\tilde{\mathbf{w}}_0$ may be written as a weighted summation of the old proper orthogonal modes and proper orthogonal coordinate histories, but the proper orthogonal values are recalculated to express the new level of participation of each proper orthogonal mode in the new response:

$$\tilde{\mathbf{W}} \approx \sum_{i=1}^{k} \tilde{\sigma}_i \mathbf{u}_i \mathbf{v}_i^{\mathrm{T}}. \tag{16}$$

Ref. [8] shows how the new proper orthogonal values may be calculated from the new initial displacement profile:

$$\tilde{\sigma}_i = \frac{\mathbf{u}_i^{\mathrm{T}} \tilde{\mathbf{w}}_0}{\mathbf{v}_{i,0}}, \quad i = 1, 2, \ldots, k. \tag{17}$$

In Eq. (17), the terms $v_{i,0}$ are the initial values of each proper orthogonal coordinate history, i.e. the first row terms in each column of $\mathbf{V}$.

Similarly, if the snapshot matrix $\mathbf{W}$ is formed from the response to an initial velocity profile $\dot{\mathbf{w}}_0$, then the snapshot matrix for the response to a new initial velocity profile $\dot{\tilde{\mathbf{w}}}_0$ may be written in the same form as Eq. (16), but the proper orthogonal values are recalculated from the new initial velocity profile as

$$\tilde{\sigma}_i = \frac{\mathbf{u}_i^{\mathrm{T}} \dot{\tilde{\mathbf{w}}}_0}{\dot{v}_{i,0}}, \quad i = 1, 2, \ldots, k. \tag{18}$$

The initial time derivatives of the proper orthogonal coordinate histories may be found from the original proper orthogonal values and the original initial velocity profile:

$$\dot{v}_{i,0} = \frac{\mathbf{u}_i^{\mathrm{T}} \dot{\mathbf{w}}_0}{\sigma_i}, \quad i = 1, 2, \ldots, k. \tag{19}$$

Now, we will use the expression for proper orthogonal coordinate histories developed to explain how the free response method from Allison et al. [8] assumes that the system's matrices $\mathbf{\Phi}_{11}(t)$ and $\mathbf{\Phi}_{12}(t)$ are diagonal. If we assume that the original response was formed by imposing an initial displacement on the structure then the expression for the scaled proper orthogonal coordinate histories is quite simple:

$$\mathbf{v}(t) = \mathbf{\Phi}_{11}(t)\mathbf{v}(0). \tag{20}$$

If we assume that $\mathbf{\Phi}_{11}(t)$ is diagonal (a valid assumption if the conditions outlined in the previous section are met) then the expression is simplified even more and a single scaled proper orthogonal coordinate history can be written as

$$v_j(t) = \mathbf{\Phi}_{11,j}(t) v_j(0) \tag{21}$$

or in time-sampled form at all time steps as

$$\hat{\mathbf{v}}_j = \sigma_j \mathbf{v}_j = \phi_{11,j} \hat{v}_{j,0}, \tag{22}$$

where $\phi_{11,j}$ is a vector containing the values of the jth diagonal element of $\mathbf{\Phi}_{11}(t)$ at every time step and the hat notation indicates that the proper orthogonal coordinate history $\mathbf{v}_j$ is scaled by its corresponding proper orthogonal value. The proper orthogonal coordinate history may be modified to represent the response to a new initial condition:

$$\tilde{\hat{\mathbf{v}}}_j = \underline{\phi}_{11,j} \tilde{\hat{v}}_{j,0} = \frac{\sigma_j \mathbf{v}_j \tilde{\hat{v}}_{j,0}}{\hat{v}_{j,0}}. \tag{23}$$

The initial values for the scaled proper orthogonal coordinate histories are related to the initial displacement profiles through a proper orthogonal mode:

$$[\, \hat{v}_{j,0} \quad \tilde{\hat{v}}_{j,0} \,] = \mathbf{u}_j^{\mathrm{T}} [\, \mathbf{w}_0 \quad \tilde{\mathbf{w}}_0 \,]. \tag{24}$$

Finally, we may insert Eq. (24) into Eq. (23) to rewrite the modified proper orthogonal coordinate history as

$$\tilde{\hat{\mathbf{v}}}_j = \sigma_j \mathbf{v}_j \frac{\mathbf{u}_j^{\mathrm{T}} \tilde{\mathbf{w}}_0}{\mathbf{u}_j^{\mathrm{T}} \mathbf{w}_0} = \sigma_j \mathbf{v}_j \frac{\tilde{\sigma}_j}{\sigma_j} = \tilde{\sigma}_j \mathbf{v}_j, \tag{25}$$

where $\tilde{\sigma}_j$ is the new proper orthogonal value obtained from Eq. (17). Eqs. (21)–(25) show that the free response method presented in Ref. [8] assumes that the modal matrices in Eq. (8) are diagonal, although this assumption was not obvious from the formulation of the method in Ref. [8]. It is trivial to show that the same assumption is made for initial velocity profiles.

3.3. Forced response identification

Now we will discuss systems that are strictly forced, i.e. systems that start at rest and are excited by an applied force $f(x, t)$. Reference [9] shows that the response to a new force $\tilde{f}(x,t)$ may be computed by modifying the proper orthogonal coordinate histories to remove the effects of the original force and incorporate the effects of the new force. If the system's mass, damping, and stiffness matrices are diagonalized by the proper orthogonal modes, then the scaled proper orthogonal coordinate histories are equal to the time-sampled results of a convolution operation:

$$v_i(t) = \int_0^t C_{ii}(t-\tau)q_i(\tau)\,\mathrm{d}\tau = C_{ii}(t) * q_i(t), \quad i = 1, 2, \ldots, k. \tag{26}$$

In Eq. (9) the terms $T_i(t)$ are continuous forms of the proper orthogonal coordinate histories $\mathbf{v}_i$, the terms $C_{ii}(t)$ are the diagonals of the time-varying matrix product $\mathbf{\Phi}_{12}(t)\mathbf{M}^{-1}(t)$, and the terms $q_i(t)$ are modal forces formed from the inner product of each proper orthogonal mode and the applied load. The terms $C_{ii}(t)$ can be considered as (proper orthogonal) modal impulse response functions. In discrete form, Eq. (26) becomes

$$\hat{v}_i(t_j) = \Delta t \sum_{p=1}^{j} C_{ii}(t_p) q_i(t_{j-p+1}), \quad i = 1, 2, \ldots, k. \tag{27}$$

We may perform the operation in Eq. (27) for every time step and write it in matrix form as

$$\hat{\mathbf{v}}_i = \Delta t \check{\mathbf{Q}}_i \mathbf{c}_{ii}, \quad i = 1, 2, \ldots, k, \tag{28}$$

where $\check{\mathbf{Q}}_i$ is a lower triangular Toeplitz matrix:

$$\check{\mathbf{Q}}_i = \begin{bmatrix} q_1(t_1) & 0 & 0 & \cdots & 0 \\ q_1(t_2) & q_1(t_1) & 0 & \cdots & 0 \\ q_1(t_3) & q_1(t_2) & q_1(t_1) & \cdots & 0 \\ \vdots & \vdots & & \ddots & \vdots \\ q_1(t_n) & q_1(t_{n-1}) & \cdots & q_1(t_2) & q_1(t_1) \end{bmatrix}_{n \times n}. \tag{29}$$

The discrete form of each modal impulse response function may be computed as

$$\mathbf{c}_{ii} = \frac{1}{\Delta t} \check{\mathbf{Q}}_i^{-1} \hat{\mathbf{v}}_i, \quad i = 1, 2, \ldots, k. \tag{30}$$

In cases where $\check{\mathbf{Q}}_i$ is rank deficient, an acceptable least squares solution may be obtained by using the Moore–Penrose pseudoinverse in place of the inverse in Eq. (30) [18].

Once the desired number of discrete modal impulse responses have been found then we may use them to predict the response to a new forcing function $\tilde{f}(x,t)$. First, we discretize $\tilde{f}(x,t)$ by writing it as a force snapshot matrix $\tilde{\mathbf{F}}$:

$$\tilde{\mathbf{F}} = \begin{bmatrix} f_1(t_1) & f_1(t_2) & \cdots & f_1(t_n) \\ f_2(t_1) & f_2(t_2) & & \\ \vdots & & \ddots & \\ f_m(t_1) & & & f_m(t_n) \end{bmatrix}, \tag{31}$$

where $f_i(t_j)$ denotes the load applied at the ith degree of freedom at time t_j. The new modal forces are then calculated

$$\tilde{\mathbf{q}}_i = \mathbf{u}_i^{\mathrm{T}}\tilde{\mathbf{F}}, \quad i = 1, 2, \ldots, k \tag{32}$$

and the new scaled proper orthogonal coordinate histories are written as

$$\hat{\tilde{\mathbf{v}}}_i = \Delta t \check{\tilde{\mathbf{Q}}}_i \mathbf{c}_{ii}, \quad i = 1, 2, \ldots, k, \tag{33}$$

where $\check{\tilde{\mathbf{Q}}}_i$ is a revised Toeplitz matrix formed from $\tilde{\mathbf{q}}_i$ as in Eq. (29). Finally, the new response is approximated as

$$\tilde{\mathbf{W}} \approx \sum_{i=1}^{k} \mathbf{u}_i \hat{\tilde{\mathbf{v}}}_i^{\mathrm{T}}. \tag{34}$$

There are several sources of error in the prediction methods explained for both strictly free and strictly forced systems. First, each method can only accurately predict a response matrix that may be spanned by the original set of proper orthogonal modes. If initial conditions or loads are introduced that generate a response that cannot be expressed by the proper orthogonal modes $\mathbf{u}_i$ then the prediction will be inaccurate. Therefore, when constructing the model it is desirable to use a response containing a wide variety of shapes in order to generate proper orthogonal modes that can represent responses to a large selection of initial conditions or loads.

Both the free- and forced-response methods assume that the modal matrices of the system are diagonalized by the proper orthogonal modes. This condition is only fully met if the structure (1) is lightly damped with a mass matrix proportional to the identity matrix and (2) is responding to an initial condition. Although many structures are lightly damped, the mass matrix condition is generally not satisfied by real structural models, and the methods are applied to forced systems as well as unforced systems. However, in many cases the proper orthogonal modes may give modal matrices that are diagonally dominant and the method may still provide an accurate response approximation.

When the method is applied to nonlinear systems, a linear time-varying model is obtained that will be able to reconstruct the original nonlinear responses accurately. For nonlinear systems, a new excitation can result in a significant change in the natural frequencies of the system and cause the system exhibit new behaviors [3,19]. The reduced-order model constructed from the proper orthogonal decomposition will be unable to predict nonlinear effects that are not present in the original signals. However, the model may accurately predict a response that is 'nearby' the original ones.

4. Adaptation for mixed responses

The previous section reviewed methods for using strictly free or forced responses of a system to predict new free or forced responses, but the methods could not be combined, i.e. a measured free response could not be used to predict a forced response or vice versa. This section describes a method for using measured mixed responses of a system to form a predictive model for both free and forced responses. First, we measure three distinct sets of response data that all result from combinations of both applied loads and initial conditions. The data are arranged in snapshot matrices ${}^a\mathbf{W}$, ${}^b\mathbf{W}$ and ${}^c\mathbf{W}$. We now calculate the proper orthogonal decomposition of the first snapshot matrix:

$${}^a\mathbf{W} \approx ({}^a\mathbf{U})({}^a\Sigma)({}^a\mathbf{V}^{\mathrm{T}}) = ({}^a\mathbf{U})({}^a\hat{\mathbf{V}}^{\mathrm{T}}). \tag{35}$$

In Eq. (35) we have combined the proper orthogonal values with the proper orthogonal coordinate histories. Eq. (35) is an approximation because we have kept only the k dominant proper orthogonal modes. We may approximate the snapshot matrix ${}^b\mathbf{W}$ using the first set of proper orthogonal modes as

$${}^b\mathbf{W} \approx ({}^a\mathbf{U})({}^a\mathbf{U}^{\mathrm{T}})({}^b\mathbf{W}), \tag{36}$$

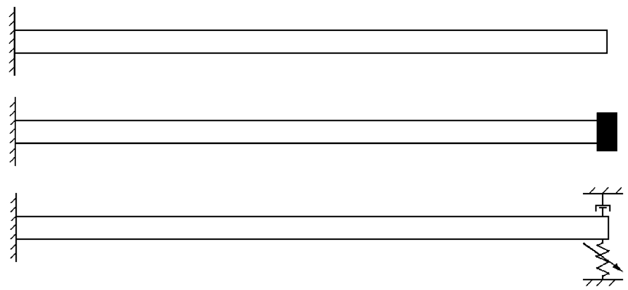

Fig. 2. Linear time-invariant (top), linear time-varying (middle), and nonlinear (bottom) beam models.

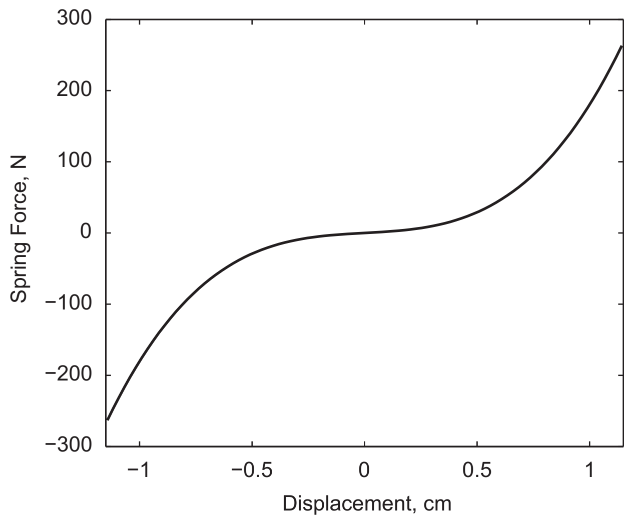

Fig. 3. Cubic spring force for nonlinear beam model.

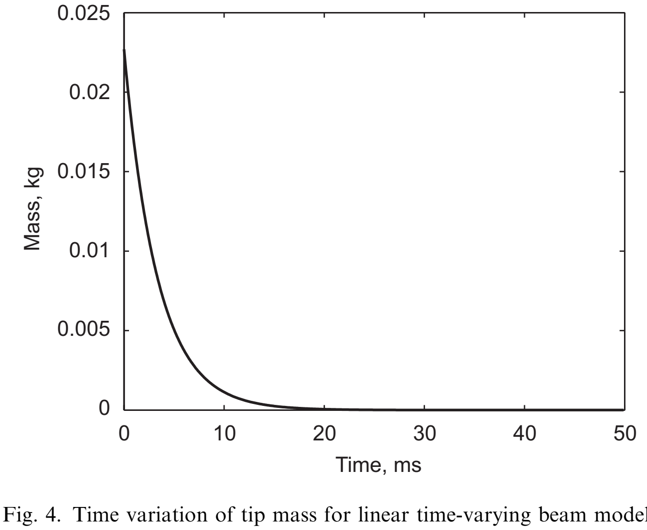

Fig. 4. Time variation of tip mass for linear time-varying beam model.

where the approximation is now transformed into the subspace spanned by the proper orthogonal modes ${}^{a}\mathbf{U}$. We may rewrite Eq. (36) as

$$ {}^{b}\mathbf{W} \approx ({}^{a}\mathbf{U})({}^{b}\hat{\mathbf{V}}^{\mathrm{T}}), \tag{37} $$

where ${}^b\hat{\mathbf{V}}^{\mathrm{T}}$ contains the time modulations of the proper orthogonal modes ${}^a\mathbf{U}$ in the response ${}^b\mathbf{W}$. Similarly, ${}^c\mathbf{W}$ can be approximated by

$$ {}^c\mathbf{W} \approx ({}^c\mathbf{U})({}^c\hat{\mathbf{V}}^{\mathrm{T}}), \tag{38}$$

where

$$ {}^c\hat{\mathbf{V}}^{\mathrm{T}} = ({}^a\mathbf{U}^{\mathrm{T}})({}^c\mathbf{W}). \tag{39}$$

Using the proper orthogonal decomposition-based identification methods outlined in the previous section, we now write each proper orthogonal coordinate history as a superposition of free and forced responses:

$$ {}^a\hat{\mathbf{v}}_i = {}^a\sigma_{i,\mathrm{disp}}\mathbf{v}_{i,\mathrm{disp}} + {}^a\sigma_{i,\mathrm{vel}}\mathbf{v}_{i,\mathrm{vel}} + {}^a\breve{\tilde{\mathbf{Q}}}_i\mathbf{c}_{ii}, \tag{40}$$

$$ {}^b\hat{\mathbf{v}}_i = {}^b\sigma_{i,\mathrm{disp}}\mathbf{v}_{i,\mathrm{disp}} + {}^b\sigma_{i,\mathrm{vel}}\mathbf{v}_{i,\mathrm{vel}} + {}^b\breve{\tilde{\mathbf{Q}}}_i\mathbf{c}_{ii}, \tag{41}$$

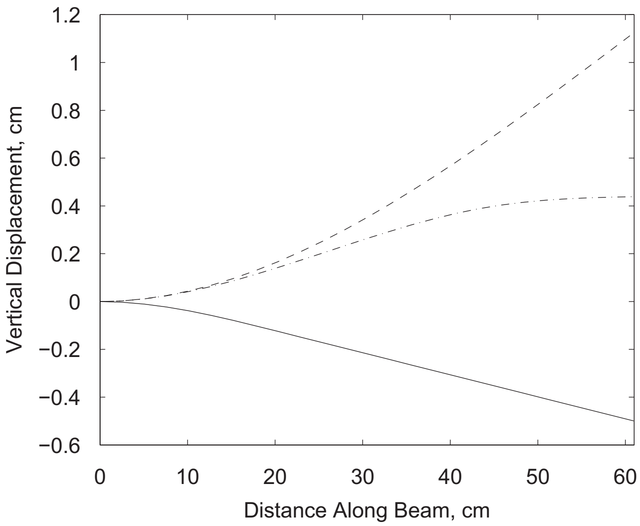

Fig. 5. Initial displacements in excitation sets a, b, and c. —— ${}^a\mathbf{w}_0$; - - - - - ${}^b\mathbf{w}_0$; - · - · - · ${}^c\mathbf{w}_0$.

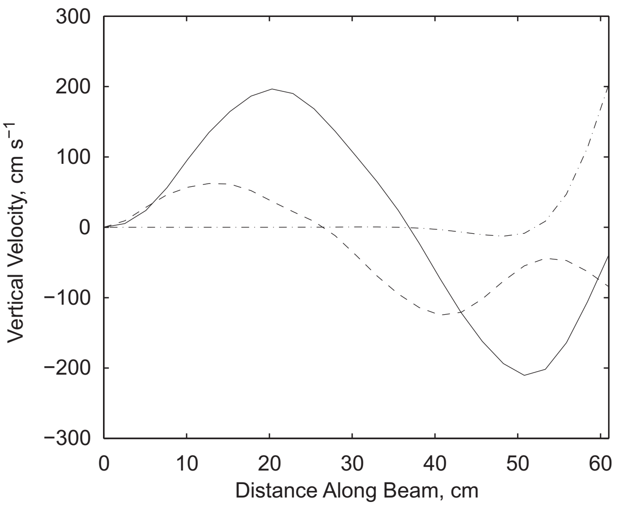

Fig. 6. Initial velocities in excitation sets a, b, and c. —— ${}^a\mathbf{w}_0$; - - - - - ${}^b\mathbf{w}_0$; - · - · - · ${}^c\mathbf{w}_0$.

$$ {}^{c}\hat{\mathbf{v}}_i = {}^{c}\sigma_{i,\mathrm{disp}}\mathbf{v}_{i,\mathrm{disp}} + {}^{c}\sigma_{i,\mathrm{vel}}\mathbf{v}_{i,\mathrm{vel}} + {}^{c}\breve{\tilde{\mathbf{Q}}}_i\mathbf{c}_{ii}. \tag{42} $$

The modal forces used to form the matrices ${}^{a}\breve{\tilde{\mathbf{Q}}}_i$, ${}^{b}\breve{\tilde{\mathbf{Q}}}_i$ and ${}^{c}\breve{\tilde{\mathbf{Q}}}_i$ are all computed using the proper orthogonal modes ${}^{a}\mathbf{U}$. The terms $\mathbf{v}_{i,\mathrm{disp}}$ and $\mathbf{v}_{i,\mathrm{vel}}$ are proper orthogonal coordinate histories for calculating the response to initial displacements and velocities, respectively. The term $\mathbf{c}_{ii}$ is a discretized modal impulse response function. We wish to solve for $\mathbf{v}_{i,\mathrm{disp}}$, $\mathbf{v}_{i,\mathrm{vel}}$, and $\mathbf{c}_{ii}$ as they will allow us to predict system responses to initial displacements, initial velocities, and loads, respectively. However, Eqs. (40)–(42) represent only three equations and there are nine unknowns.

Additional equations may be found by considering the initial displacement and velocity profiles used to generate ${}^{a}\mathbf{W}$, ${}^{b}\mathbf{W}$ and ${}^{c}\mathbf{W}$. We can compute the ratio of two displacement-related proper orthogonal values as

$$ \frac{{}^{a}\sigma_{i,\mathrm{disp}}}{{}^{b}\sigma_{i,\mathrm{disp}}} = \frac{({}^{a}\mathbf{u}_i^{\mathrm{T}})({}^{a}\mathbf{w}_0)/v_{i,0,\mathrm{disp}}}{({}^{a}\mathbf{u}_i^{\mathrm{T}})({}^{b}\mathbf{w}_0)/v_{i,0,\mathrm{disp}}} = \frac{({}^{a}\mathbf{u}_i^{\mathrm{T}})({}^{a}\mathbf{w}_0)}{({}^{a}\mathbf{u}_i^{\mathrm{T}})({}^{b}\mathbf{w}_0)}. \tag{43} $$

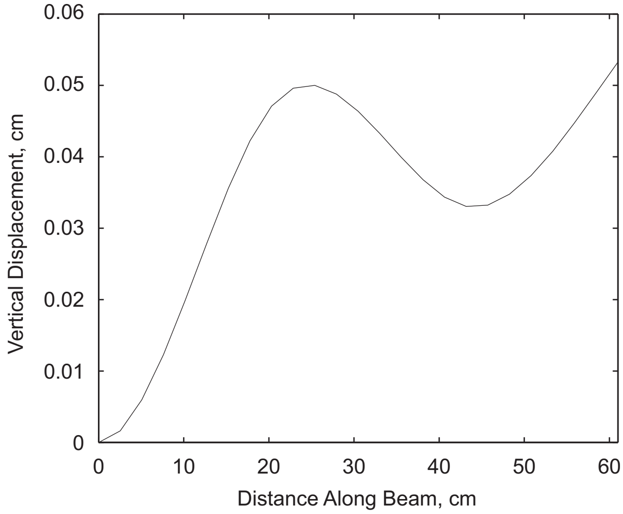

Fig. 7. New initial displacement profile $\tilde{\mathbf{w}}_0$.

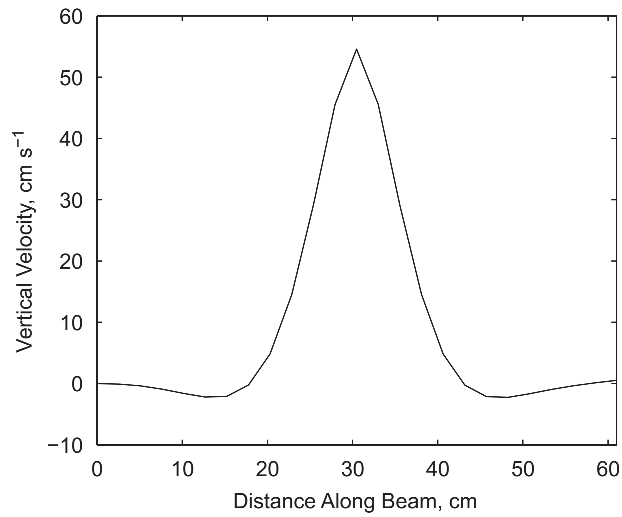

Fig. 8. New initial velocity profile $\dot{\tilde{\mathbf{w}}}_0$.

Similarly, the remaining displacement proper orthogonal value ratio and the velocity proper orthogonal value ratios can be computed as

$$\frac{{}^{a}\sigma_{i,\mathrm{disp}}}{{}^{c}\sigma_{i,\mathrm{disp}}} = \frac{({}^{a}\mathbf{u}_i^{\mathrm{T}})({}^{a}\mathbf{w}_0)}{({}^{a}\mathbf{u}_i^{\mathrm{T}})({}^{c}\mathbf{w}_0)}, \tag{44}$$

$$\frac{{}^{a}\sigma_{i,\mathrm{vel}}}{{}^{b}\sigma_{i,\mathrm{vel}}} = \frac{({}^{a}\mathbf{u}_i^{\mathrm{T}})({}^{a}\dot{\mathbf{w}}_0)}{({}^{a}\mathbf{u}_i^{\mathrm{T}})({}^{b}\dot{\mathbf{w}}_0)}, \tag{45}$$

$$\frac{{}^{a}\sigma_{i,\mathrm{vel}}}{{}^{c}\sigma_{i,\mathrm{vel}}} = \frac{({}^{a}\mathbf{u}_i^{\mathrm{T}})({}^{a}\dot{\mathbf{w}}_0)}{({}^{a}\mathbf{u}_i^{\mathrm{T}})({}^{c}\dot{\mathbf{w}}_0)}. \tag{46}$$

The final two equations are obtained by recalling the orthonormality of proper orthogonal coordinate histories:

$$\mathbf{v}_{i,\mathrm{disp}}^{\mathrm{T}}\mathbf{v}_{i,\mathrm{disp}} = 1, \tag{47}$$

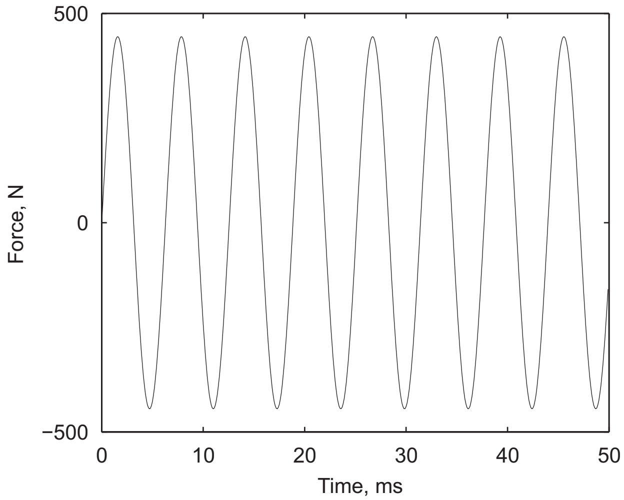

Fig. 9. New load $\tilde{\mathbf{F}}(t)$ applied vertically at beam tip.

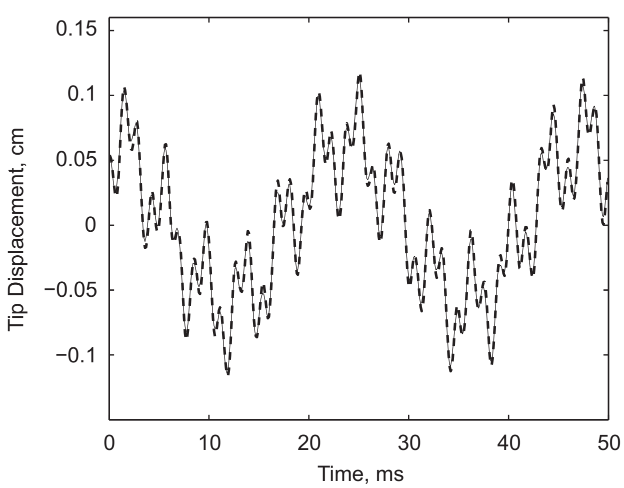

Fig. 10. Tip displacements for linear time-invariant beam in response to $\tilde{\mathbf{w}}_0$: —— finite element model and - - - - - mixed response method.

$$\mathbf{v}_{i,\mathrm{vel}}^{\mathrm{T}}\mathbf{v}_{i,\mathrm{vel}} = 1. \tag{48}$$

Eqs. (40)–(48) represent a system of linear equations that may be solved to obtain $\mathbf{v}_{i,\mathrm{disp}}$, $\mathbf{v}_{i,\mathrm{vel}}$, and $\mathbf{c}_{ii}$ for $i = 1, 2, \ldots, k$. Once these quantities are obtained they may be used as explained in the previous section to predict the response of the system to initial displacements, initial velocities, or applied loads. Because the methods in the previous section are linear, the response to a combination of these excitation types may be found by superposing the separate responses.

If mixed response data are used to predict the response to initial velocities then the method given in the previous section must be modified slightly. In the previous section the initial time derivative of each proper orthogonal coordinate history was calculated from Eq. (19). If mixed response data are used to identify $\mathbf{v}_{i,\mathrm{vel}}$ then the initial time derivative $\dot{v}_{i,0,\mathrm{vel}}$ can not be calculated in the same way because there are no proper orthogonal values directly corresponding to $\mathbf{v}_{i,\mathrm{vel}}$. In this case, however, we can approximate $\dot{v}_{i,0,\mathrm{vel}}$ as

$$\dot{v}_{i,0,\mathrm{vel}} \approx \frac{v_{i,\mathrm{vel}}(t_2) - v_{i,\mathrm{vel}}(t_1)}{\Delta t}. \tag{49}$$

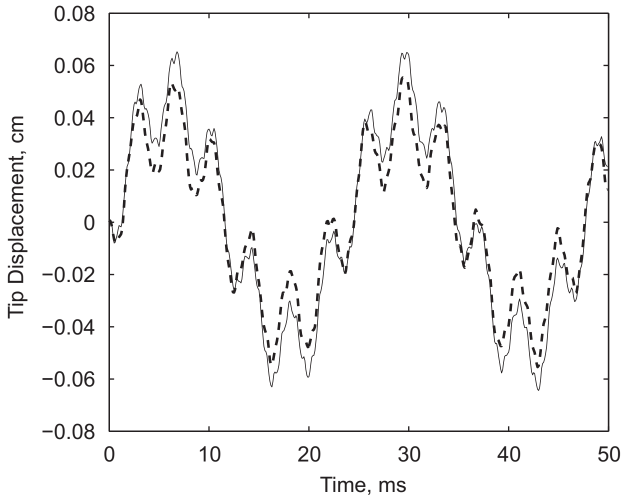

Fig. 11. Tip displacements for linear time-invariant beam in response to $\dot{\mathbf{w}}_0$: —— finite element model and - - - - - mixed response method.

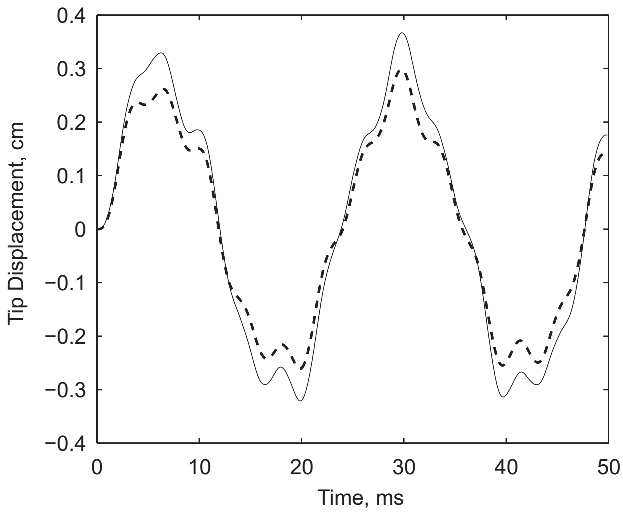

Fig. 12. Tip displacements for linear time-invariant beam in response to $\tilde{\mathbf{F}}(t)$: —— finite element model and - - - - - mixed response method.

The same types of error present in the strictly free and strictly forced response prediction methods are also present in the mixed response method given here.

5. Examples

This section applies the proposed method to three beam models, shown in Fig. 2. The first model is a linear time-invariant undamped cantilever beam. Next, a time-varying tip mass is attached to the tip of the beam to convert it to a linear time-varying system. The linear time-invariant beam is also converted to a nonlinear system by attaching a cubic spring to the tip. A dashpot is also attached to the nonlinear beam to simulate damping. All of the beam models were made of steel ($E = 2 \times 10^{11}\,\mathrm{Pa}$, $\rho = 8000\,\mathrm{kg\,m^{-3}}$) and had dimensions of $61 \times 2.54 \times 1.9\,\mathrm{cm^3}$. Finite element models were created for each beam using 24 beam elements. The spring force (over the tip displacement range seen in simulations) for the nonlinear beam is shown in Fig. 3 ($F(w_{\mathrm{tip}}) = 17.5w_{\mathrm{tip}} + 163w_{\mathrm{tip}}^3$) and the time variance in the tip mass for the linear time-varying beam is shown in Fig. 4 ($m(t) = 0.023\mathrm{e}^{-300t}$). The value of the dashpot on the nonlinear beam was $35\,\mathrm{N\,s\,in^{-1}}$.

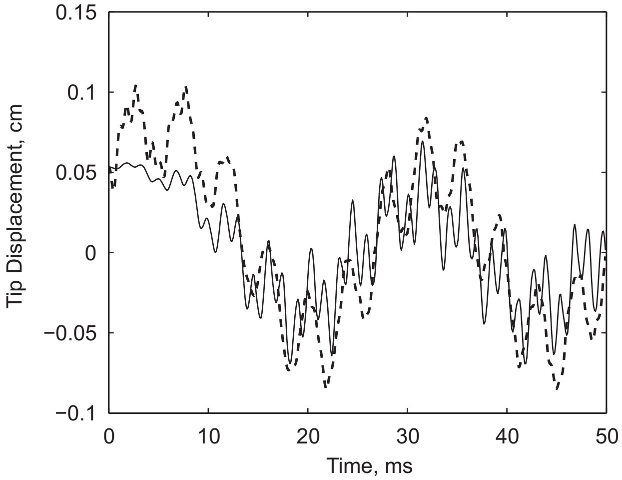

Fig. 13. Tip displacements for linear time-varying beam in response to $\tilde{\mathbf{w}}_0$: —— finite element model and ----- mixed response method.

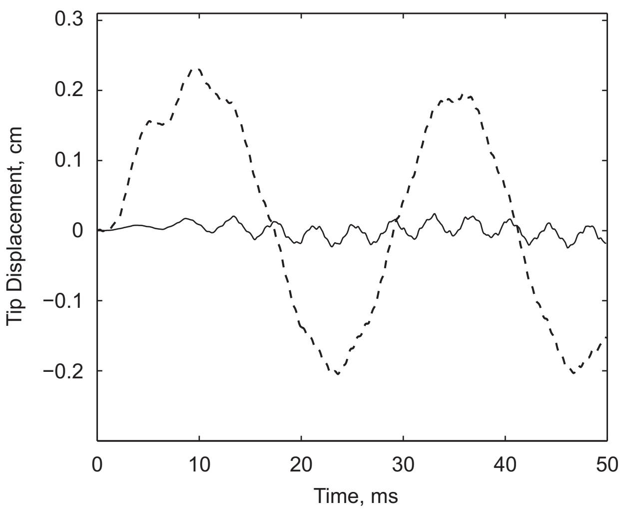

Fig. 14. Tip displacements for linear time-varying beam in response to $\dot{\tilde{\mathbf{w}}}_0$: —— finite element model and ----- mixed response method.

The Newmark method was applied to simulate the exact response of each beam model to three excitation sets consisting of initial displacements and velocities and an applied force. The initial displacement and velocity profiles for the beams are shown in Figs. 5 and 6, respectively, and a 2224 N vertical pulse was applied for 0.5 ms at locations 21, 12, and 3 in from the beam root for respective excitation sets a, b, and c. The responses of each beam model to each excitation set were simulated for 50 ms and the vertical displacements at 25 points along each beam were captured every 0.1 ms to form $\mathbf{W}$. Thus the dimensions of ${}^{a}\mathbf{W}$, ${}^{b}\mathbf{W}$ and ${}^{c}\mathbf{W}$ were (25×500) for all beam models.

Next, the proper orthogonal decomposition was computed for each beam's response to excitation set *a* and the mixed response method described in the previous sections was applied to identify $\mathbf{v}_{i,\mathrm{disp}}$, $\mathbf{v}_{i,\mathrm{vel}}$, and $\mathbf{c}_{ii}$ for each beam using excitation sets *b* and *c* as supplementary excitations. These quantities were used to simulate the response of both systems to a new initial displacement $\tilde{\mathbf{w}}_0$, a new initial velocity $\dot{\tilde{\mathbf{w}}}_0$, and a new applied load $\tilde{\mathbf{F}}(t)$, shown in Figs. 7, 8, and 9, respectively. Although responses to initial displacements, velocities, and excitations are calculated separately here, responses to mixed conditions can be obtained easily by superposing

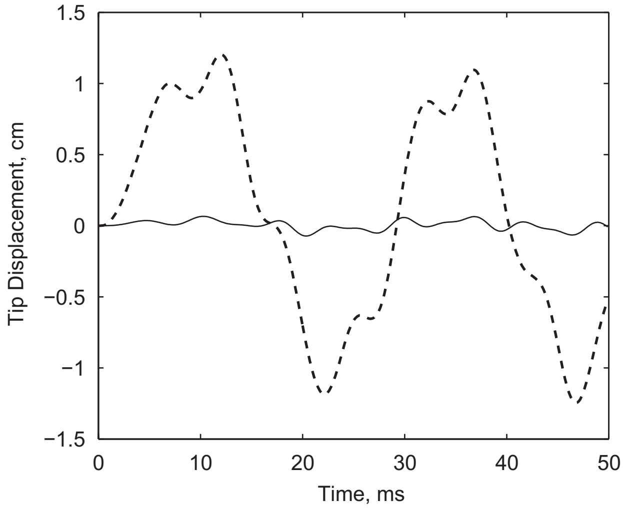

Fig. 15. Tip displacements for linear time-varying beam in response to $\tilde{\mathbf{F}}(t)$: —— finite element model and - - - - - mixed response method.

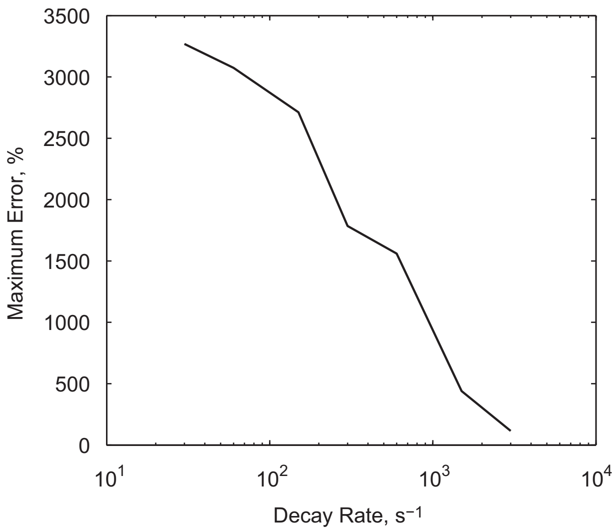

Fig. 16. Maximum error variation with tip mass decay rate.

the responses to each conditions. The responses were simulated using the first four proper orthogonal modes, which corresponded to 99% of the original signal energy.

The tip displacements at each time step calculated by the finite element model and the mixed response method for response of the linear time-invariant beam to each excitation are shown in Figs. 10–12. All three figures show that the proper orthogonal decomposition-based model predicts the tip displacements accurately for the beam, but that errors are present, particularly in the responses to $\dot{\tilde{\mathbf{w}}}_0$ and $\tilde{\mathbf{F}}(t)$. The errors may be attributed to (1) the inability of the proper orthogonal modes computed from ${}^a\mathbf{W}$ to perfectly predict the new response and (2) the fact that the modal matrices of the beam are not diagonalized by the proper orthogonal modes. Despite the errors, however, the mixed response method produces satisfactory predictions even when the proper orthogonal modes do not perfectly diagonalize the system matrices.

The tip displacements at each time step calculated by the finite element model and the mixed response method for the linear time-varying beam are shown in Figs. 13–15 for the responses to the initial displacement, initial velocity, and load, respectively. The effect of the time-varying tip mass is visible in the responses as changes in amplitude and frequency content over time. These figures show that significant errors are present in

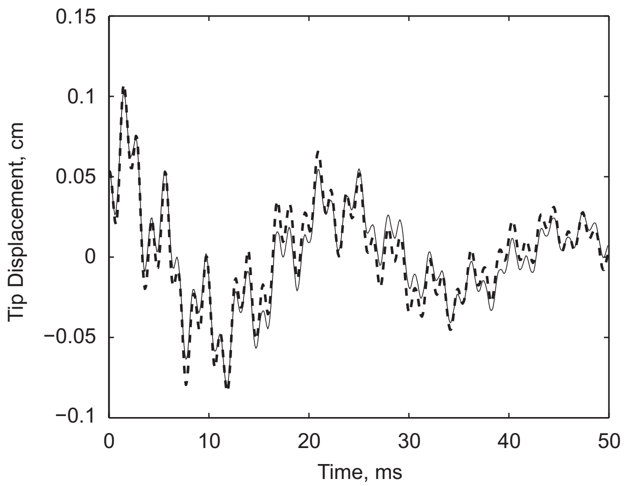

Fig. 17. Tip displacements for nonlinear beam in response to $\tilde{\mathbf{w}}_0$: —— finite element model and - - - - - mixed response method.

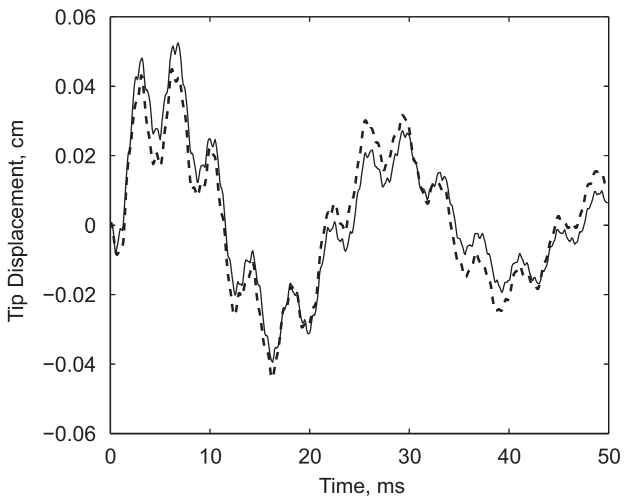

Fig. 18. Tip displacements for nonlinear beam in response to $\dot{\tilde{\mathbf{w}}}_0$: —— finite element model and - - - - - mixed response method.

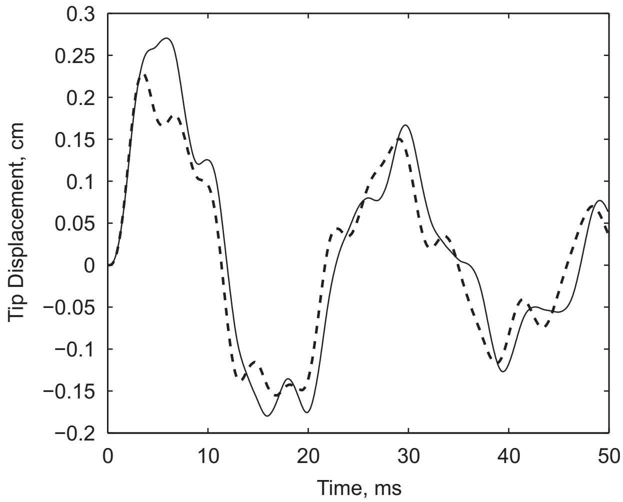

Fig. 19. Tip displacements for nonlinear beam in response to $\tilde{\mathbf{F}}(t)$: —— finite element model and ----- mixed response method.

the method's response predictions for the linear time-varying beam model for all of the excitations, particularly the response to the initial velocity and applied load. These errors are attributed to the fact that the (initially) large tip mass strongly violates the requirement that the mass matrix must be proportional to the identity matrix and the modal matrices for the system are not accurately approximated as diagonal matrices.

The negative effects of the tip mass may be increased or reduced by changing the exponential decay rate of the tip mass. If the mass decreases more slowly than shown in Fig. 4 then its negative effect on the mass matrix lasts longer and reduces the accuracy of the prediction. On the other hand, however, as the decay rate is increased then the diagonal terms on the mass matrix are similar to each other for a longer length of time, increasing the accuracy of the solution. This trend is illustrated in Fig. 16, which shows the maximum error of the mixed response method's prediction at various decay rates is shown in Fig. 16.

The displacement norms for the nonlinear beam are shown in Figs. 17–19 for the three new excitations. In each figure the results obtained using the mixed response method are plotted with the exact results obtained by the finite element model. The figures show that the method is capable of generating a reasonably accurate response prediction without requiring any information about the functional form of the nonlinearity, although several sources of error are present. As with the other beams, error is introduced from both (1) using proper orthogonal modes from a response that is different than the predicted one and (2) assuming that the matrices $\mathbf{\Phi}_{11}(t)$, $\mathbf{\Phi}_{12}(t)$, and $\mathbf{C}(t)$ are diagonal. The response predictions for the nonlinear beam contain additional errors that result from using a linear time-varying method for identifying a nonlinear system. The linear model, although able to reproduce the original nonlinear data sets, exhibits frequency and magnitude discrepancies when predicting the new responses. Frequency discrepancies are most visible in the response to $\tilde{\mathbf{F}}(t)$.

6. Conclusions

The results displayed in the previous section demonstrate that the proposed method is capable of producing accurate response predictions for models whose modal matrices are approximately diagonalized by the proper orthogonal modes. Although the example analyses shown were performed with finite element models, the results suggest that the proposed method may be applied to construct an accurate predictive model for a structure from data obtained by time sampling the transient response of the structure in an experiment.

This paper outlined a method for using the proper orthogonal decomposition with linear system theory to construct a linear time-varying model for a structure by measuring its response to any combination of applied loads or initial conditions. The model is formed by combining previous methods for creating proper orthogonal decomposition-based models from strictly free or forced responses of the system. No knowledge of the governing equations of motion for the structure (e.g., from a finite element model) is required to construct the model. Thus, the proposed method may provide a useful technique for modeling nonlinear systems using only test data when the form of the nonlinearity is unknown. For linear systems the accuracy of the method depends on (1) how well the proper orthogonal modes from the original response span the space of the predicted response and (2) how well the proper orthogonal modes diagonalize the modal matrices for the system. For nonlinear systems the same conditions are important but additional error may be present if the frequency content or nonlinear characteristics of the predicted response are significantly different from those available in the measured data.

Acknowledgments

The first author acknowledges support from a National Physical Science Consortium fellowship, a Virginia Space Grant Consortium fellowship, and stipend support from Sandia National Laboratories. The third author acknowledges support from the George R. Goodson Professorship.

References

[1] K.H. Huebner, T.G. Byrom, D.L. Dewhirst, D.E. Smith, *The Finite Element Method for Engineers*, Wiley, New York, 2001.
[2] J.K. Bennighof, M.B. Muller, M.F. Kaplan, Computational costs for large structure frequency response methods, *Proceedings of the 38th AIAA Structures, Structural Dynamics, and Materials Conference*, Kissimmee, April 1997, Paper 1977-1274.
[3] G. Kerschen, K. Worden, A.F. Vakakis, J.C. Golinval, Past, present and future of nonlinear system identification in structural dynamics, *Mechanical Systems and Signal Processing* 20 (2006) 505–592.
[4] D.J. Ewins, *Modal Testing: Theory and Practice*, Research Studies Press Ltd., Hertfordshire, 1984.
[5] M. Friswell, J.E. Mottershead, *Finite Element Model Updating in Structural Dynamics (Solid Mechanics and its Applications)*, Kluwer, Dordrecht, 1995.
[6] M. Verhaegen, X. Yu, A class of subspace model identification algorithms to identify periodically and arbitrarily linear time-varying systems, *Automatica* 31 (1995) 201–216.
[7] J.B. MacNeil, R.E. Kearney, I.W. Hunter, Identification of time-varying biological systems from ensemble data [joint dynamics application], *IEEE Transactions on Biomedical Engineering* 39 (1992) 1213–1225.
[8] T.C. Allison, A.K. Miller, D.J. Inman, Free response simulation via the proper orthogonal decomposition, *AIAA Journal* 45 (2007) 2538–2543.
[9] T.C. Allison, A.K. Miller, D.J. Inman, A deconvolution-based approach to structural dynamics system identification and response prediction, *ASME Journal of Vibration and Acoustics* 130 (2008) 031010.
[10] G. Kerschen, J.C. Golinval, A.F. Vakakis, L.A. Bergman, The method of proper orthogonal decomposition for dynamical characterization and order reduction of mechanical systems: an overview, *Nonlinear Dynamics* 41 (2005) 147–169.
[11] G. Berkooz, P. Homes, J.L. Lumley, The proper orthogonal decomposition in the analysis of turbulent flows, *Annual Review of Fluid Mechanics* 25 (1993) 539–575.
[12] R. Kappagantu, B.F. Feeny, An optimal modal reduction of a system with frictional excitation, *Journal of Sound and Vibration* 224 (1999) 863–877.
[13] B.F. Feeny, R. Kappagantu, On the physical interpretation of proper orthogonal modes in vibrations, *Journal of Sound and Vibration* 211 (1998) 607–616.
[14] G. Kerschen, J.C. Golinval, Physical interpretation of the proper orthogonal modes using the singular value decomposition, *Journal of Sound and Vibration* 249 (2002) 849–865.
[15] B.F. Feeny, On the proper orthogonal modes and normal modes of continuous vibration systems, *Journal of Vibration and Acoustics* 124 (2002) 157–160.
[16] L. Meirovitch, *Principles and Techniques of Vibrations*, Prentice-Hall, New Jersey, 1997.
[17] J.J. Dacunha, Transition matrix and generalized matrix exponential via the Peano–Baker series, *Journal of Difference Equations and Applications* 11 (2005) 1245–1264.
[18] J. Rahman, T.K. Sarkar, Deconvolution and total least squares in finding the impulse response of an electromagnetic system from measured data, *IEEE Transactions on Antennas and Propagation* 43 (1995) 416–421.
[19] L.N. Virgin, *Introduction to Experimental Nonlinear Dynamics: A Case Study in Mechanical Vibration*, Cambridge University Press, New York, 2000.